Dewetting Behavior of a Block Copolymer/Homopolymer Thin Film on an Immiscible Homopolymer Substrate

ARTICLE *in* LANGMUIR · OCTOBER 2004

Impact Factor: 4.46 · DOI: 10.1021/la049562c · Source: PubMed

3 AUTHORS, INCLUDING:

Richard J Spontak
North Carolina State University
245 PUBLICATIONS **5,930** CITATIONS

SEE PROFILE

Dewetting Behavior of a Block Copolymer/Homopolymer Thin Film on an Immiscible Homopolymer Substrate

Bin Wei,[†] Jan Genzer,*[,†] and Richard J. Spontak[†,‡]

Departments of Chemical Engineering and Materials Science and Engineering, North Carolina State University, Raleigh, North Carolina 27695

Received February 19, 2004. In Final Form: June 9, 2004

Numerous previous studies have established that the addition of a microphase-ordered AB diblock copolymer to a thin homopolymer A (hA) film can slow, if not altogether prevent, film rupture and subsequent film dewetting on a hard substrate such as silica. However, only a few reports have examined comparable phenomena when the hA/AB blend resides on a soft B-selective surface, such as homopolymer B (hB). In this work, the dewetting kinetics of thin films composed of polystyrene (PS) and a symmetric poly(styrene-*b*-methyl methacrylate) (SM) diblock copolymer on a poly(methyl methacrylate) substrate is investigated by hot-stage light microscopy. Without the SM copolymer, the dewetting rate of the PS layer is constant under isothermal conditions and exhibits Arrhenius behavior with an apparent activation energy of ∼180 kJ/mol. Addition of the copolymer promotes a crossover from early- to late-stage dewetting kinetics, as evidenced by measurably different dewetting rates. Transmission electron microscopy reveals the morphological characteristics of dewetted PS/SM films as functions of film thickness and SM concentration.

Introduction

The dewetting of a homopolymer thin film on a substrate has remained a subject of considerable research interest over the past decade due to the considerable importance of this topic in both practical applications and theoretical investigations.[1−15] In a wide variety of commercial technologies, a thorough understanding of dewetting phenomena is crucial for the expedient development of stable coatings.[5,6] From a theoretical standpoint, the typically high viscosity of macromolecules provides relevant time scales that are readily accessible in the dynamic experiments required for guidance and verification. Most research efforts reported[1−3,7−9] to date have focused on the dewetting of polymer thin films on a hard (impenetrable) surface and have consequently established that the spreading parameter (S), defined in eq 1 below, constitutes the key measure to discern whether dewetting occurs:[6]

$$S = \gamma_B - (\gamma_A + \gamma_{AB}) \tag{1}$$

In eq 1, γ_A and γ_B represent the surface tension of the polymer layer (A) and the substrate (B), respectively, and γ_{AB} is the interfacial tension at the A/B interface. When $S > 0$, layer A remains stable and does not dewet. If $S < 0$, however, layer A becomes unstable, ruptures, and dewets from substrate B through the formation of holes. Material excavated from a hole tends to accumulate around the hole to produce a well-defined rim. As the hole grows with increasing time, the rim impinges into the rims of neighboring holes so that the ruptured film develops a contiguous dewetting pattern. Further annealing causes the rims to break into discrete droplets due to Rayleigh instability.[7] When equilibrium is ultimately achieved, the droplets become spherical and exhibit a contact angle described by the Young[10,16] equation, viz.,

$$\cos \theta_E = (\gamma_B - \gamma_{AB})/\gamma_A \tag{2}$$

where θ_E is the Neumann contact angle, i.e., the angle formed by the liquid edge at the three-phase contact line.

The dewetting of a liquid film on the surface of another liquid constitutes a much more complicated physical process[2,4,6,11,12] relative to analogous dewetting on a solid substrate. In this case, the interface between the dewetting layer and the substrate is no longer restrained to remain flat. At equilibrium, droplets of the dewetted layer adopt a lens-like, rather than spherical, shape. Under these conditions, S can again be determined by balancing the interfacial tensions at the three-phase contact line to yield[6]

$$S = -\gamma\, \theta_E^2/2 \tag{3}$$

where γ is an effective surface tension defined as $(1/\gamma_A + 1/\gamma_B)^{-1}$. Brochard-Wyart et al.[12] have conducted a theoretical study of liquid−liquid dewetting dynamics between

* To whom correspondence should be addressed. E-mail: jan_genzer@ncsu.edu.

[†] Department of Chemical Engineering, North Carolina State University.

[‡] Department of Materials Science and Engineering, North Carolina State University.

(1) Karapanagiotis, I.; Evans, D. F.; Gerberich, W. W. *Colloid Surf., A* **2002**, *207*, 59.

(2) Redon, C.; Brochard-Wyart, F.; Rondelez, F. *Phys. Rev. Lett.* **1991**, *66*, 715.

(3) Brochard-Wyart, F.; Debregeas, G.; Fondecave, R.; Martin, P. *Macromolecules* **1997**, *30*, 1211.

(4) Faldi, A.; Composto, R. J.; Winey, K. I. *Langmuir* **1995**, *11*, 4855.

(5) Geoghegan, M.; Krausch, G. *Prog. Polym. Sci.* **2003**, *28*, 261.

(6) Krausch, G. *J. Phys.: Condens. Matter* **1997**, *9*, 7741.

(7) Sharma, A.; Reiter, G. *J. Colloid Interface Sci.* **1996**, *178*, 383.

(8) Müller-Buschbaum, P.; Gutmann, J. S.; Stamm, M.; Cubitt, R.; Cunis, S.; von Krosigk, G.; Gehrke, R.; Petry, W. *Physica B* **2000**, *283*, 53.

(9) Müller-Buschbaum, P.; Gutmann, J. S.; Lorenz-Haas, C.; Wunnicke, O.; Stamm, M.; Petry, W. *Macromolecules* **2002**, *35*, 2017.

(10) Vitt, E.; Shull, K. R. *Macromolecules* **1995**, *28*, 6349.

(11) Lambooy, P.; Phelan, K. C.; Haugg, O.; Krausch, G. *Phys. Rev. Lett.* **1996**, *76*, 1110.

(12) Brochard-Wyart, F.; Martin, P.; Redon, C. *Langmuir* **1993**, *9*, 3682.

(13) Costa, A. C.; Composto, R. J.; Vlček, P. *Macromolecules* **2003**, *36*, 3254.

(14) Hamley, I. W.; Hiscutt, E. L.; Yang, Y. W.; Booth, C. *J. Colloid Interface Sci.* **1999**, *209*, 255.

(15) Harris, M.; Appel, G.; Ade, H. *Macromolecules* **2003**, *36*, 3307.

(16) Young, T. *Philos. Trans. R. Soc. London* **1805**, *5*, 65.

10.1021/la049562c CCC: $27.50
Published on Web 08/21/2004

polymer melts. They report that the dewetting rate depends strongly on the viscosities of the dewetting liquid (η_A) and the liquid substrate (η_B). When $\eta_B > \eta_A/\theta_E$ and the liquids exhibit a relatively small contact angle, the substrate deforms slightly, while the diameter (D) of the holes in the dewetting layer is predicted[12] to grow linearly with time (t). In this case, the isothermal dewetting rate (dD/dt) is constant. If, on the other hand, $\eta_B < \eta_A/\theta_E$, the dewetting rate is expected[12] to become time-dependent.

Previous studies have elucidated the dewetting behavior of (i) a single polymer (homopolymer[7] or block copolymer[9,14]) on a solid or liquid substrate and (ii) a block copolymer/homopolymer blend[13] on a solid substrate. Although AB block copolymers are commonly employed to compatibilize their immiscible parent homopolymers (hA and hB),[17] to the best of our knowledge, there are no reports that explore the dewetting kinetics of an AB/hA blend on hB. We do, however, recognize that the recent study of Zhu et al.[18] has demonstrated that complex morphologies, such as microemulsions, can form in such confined double-layer systems. Motivated by the importance of understanding the stabilizing efficacy of copolymer-modified homopolymer films, we have examined the dewetting kinetics of a polystyrene (PS) thin film with and without a poly(styrene-*b*-methyl methacrylate) (SM) diblock copolymer on a poly(methyl methacrylate) (PMMA) substrate. This particular system is ideal for the present study since high-molecular-weight PS and PMMA are immiscible and dewet from each other at typical annealing temperatures (>160 °C and < 220 °C) due to their high interfacial tension ($\gamma_{PS/PMMA}$).[15] Over this temperature range, $\gamma_{PS/PMMA}$ is larger in magnitude than the difference in the homopolymer surface tensions ($\gamma_{PS} - \gamma_{PMMA}$). For instance, γ_{PS} and γ_{PMMA} are reported[19] to be 29.3 and 29.0 mJ/m^2, respectively, whereas $\gamma_{PS/PMMA}$ is found[20] to be 1.26 mJ/m^2, at 180 °C. To minimize the system free energy, the double-layer tends to reduce the area of the PS/PMMA interface, which promotes dewetting of the top layer in both PS/PMMA and PMMA/PS double-layer arrangements. In this work, we investigate the effect of adding a microphase-ordered SM copolymer to the upper PS layer, which is anticipated to reduce the PS/PMMA interfacial tension and ultimately stabilize the PS/SM film once a sufficient population of copolymer molecules migrates to the PS/PMMA interface.

Experimental Section

Materials. Two PS homopolymers with number-average molecular weights of 50 000 and 200 000 Da and polydispersity index (PI) values of ≤1.06 were purchased from Pressure Chemical, Inc. (Pittsburgh, PA). Two PMMA homopolymers with molecular weights of 226 000 and 281 000 Da and PI values of 1.05 or less, as well as a symmetric SM diblock copolymer with block weights of 50 000 (S) and 54 000 Da (M) and a PI of ≈1.04, were obtained from Polymer Source, Inc. (Dorval, Canada). All molecular characteristics reported herein were provided by the manufacturers. To facilitate discussion, the PS and PMMA homopolymers are hereafter designated as either PS*M* or PMMA*M*, where *M* is the number-average molecular weight in kDa. Solvent-grade toluene was supplied by Fisher Scientific (Fairlawn, NJ) and was used without further purification

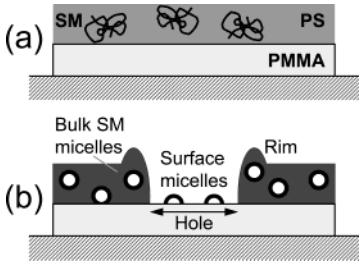

Figure 1. Illustration of the PS/SM+PMMA double-layer assemblies investigated in this work. The as-cast PS/SM layer depicted in (a) is presumed to possess a nonequilibrium morphology. Upon annealing at temperatures in the melt (b), this morphology is refined as (i) the copolymer molecules self-organize into micelles and migrate to the PS/PMMA interface and (ii) the PS top layer simultaneously dewets from the PMMA substrate. Individual SM molecules and SM micelles adsorbed to the PMMA substrate remain on the dry PMMA surface upon dewetting.

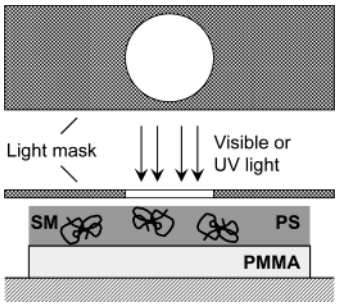

Figure 2. Schematic depiction of the hot-stage setup employed here showing the specimen area continuously illuminated by visible light or UV radiation during extended annealing times.

Methods. Thin polymer films employed throughout the course of this study were prepared by spin-coating from toluene solutions. Each PMMA film, ~50 nm thick, was directly spin-coated onto a solid substrate: either a silicon wafer with its native oxide intact or rocksalt for analysis by transmission electron microscopy (TEM). Films of PS or PS/SM blends varying in thickness from 20 to 100 nm were spin-coated onto glass microscope slides. The mass fraction of SM copolymer in the PS layer (W_{SM}) ranged from 0.00 (pure PS) to 0.48. The resultant PS or PS/SM films were floated onto deionized water and picked up on the top of a PMMA film to form a double-layer film, as illustrated in Figure 1. After drying in air at ambient temperature for at least 24 h, the samples were annealed at predesignated temperatures (175−190 °C) well above the glass transition temperature (T_g) of both PS (~100 °C) and PMMA (~120 °C, corresponding to the 79% syndiotacticity[21] information provided by the manufacturer). Annealing was performed in either a high vacuum oven (≈10^{-7} Torr), a moderately high-vacuum chamber attached to a diffusion pump (≈10^{-4} Torr), or a Mettler-Toledo hot-stage under a circulating N_2 blanket. Dewetting kinetics were monitored at various temperatures in situ with an Olympus BX60 optical microscope equipped with a computer-interfaced CCD camera and operated in reflection mode. In some cases, specimens within the hot-stage were continuously exposed to visible or UV light for extended periods of time (see Figure 2). After annealing at specific temperatures for an equilibration period of 7 days, the double-layer assemblies prepared on rock salt were floated onto copper TEM grids, exposed to the vapor of 0.5% RuO_4(aq) for 7 min and examined on a Zeiss EM902 electron spectroscopic microscope operated at 80 kV and an energy loss of 0 eV. Atomic force microscopy (AFM, operated in tapping mode) and profilometry of selected surface topologies that developed upon annealing were performed on Digital Instruments 3000 and Alpha-step500 instruments, respectively.

(17) Spontak, R. J.; Patel, N. P. In *Developments in Block Copolymer Science and Technology*; Hamley, I. W., Ed.; Wiley: New York, 2004; Chapter 5.

(18) Zhu, S.; Liu, Y.; Rafailovich, M. H.; Sokolov, J.; Gersappe, D.; Winesett, D. A.; Ade, H. *Nature* **1999**, *400*, 49.

(19) Wu, S. *Polymer Interface and Adhesion*; Marcel Dekker: New York, 1982.

(20) Carriere, C. J.; Biresaw, G.; Sammler, R. L. *Rheol. Acta* **2000**, *39*, 476.

(21) *Polymer Handbook*, 4 ed.; Brandrup, J., Immergut, E. H., Grucke, E. A., Eds.; Wiley & Sons: New York, 1999.

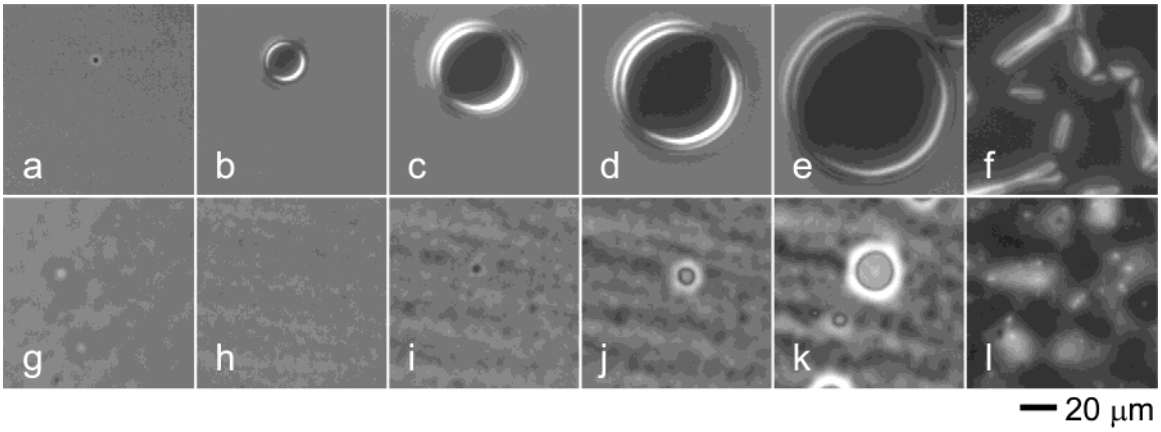

Figure 3. Series of optical microscopy images (using phase-contrast and Nomarski optics) of PS200/SM layers on PMMA281 acquired at different times, annealing temperatures, and copolymer concentrations. In (a−f), the annealing temperature of neat PS200 is held constant at 175 °C, while the annealing time (in hours) is varied: (a) 4.6, (b) 22, (c) 49, (d) 70, (e) 96, and (f) 145. The image displayed in (g) is collected from a PS200/SM layer with $W_{SM} = 0.12$ after being annealed at 175 °C for 181 h. In (h−l), the annealing temperature and copolymer concentration are constant at 180 °C and 0.12, respectively, and the annealing time (in hours) is varied: (h) 23, (i) 47, (j) 71, (k) 96, and (l) 144.

Results and Discussion

Film Stability and Dewetting Kinetics. Thin films of PS50 and PS200 homopolymers measuring ∼67 nm are not stable and spontaneously dewet from PMMA when the double-layer assembly is annealed at temperatures above 175 °C. Addition of the SM block copolymer to the PS layer is found to generally enhance the overall stability of the upper layer. The stability of the films depends on several factors, such as block copolymer concentration (W_{SM}), film thickness (L), and PS molecular weight. In those instances when a PS/SM blend showed evidence of dewetting, the rate at which dewetting proceeded (dD/dt) is measured to be substantially slower than that of the neat PS. In the remainder of this section, the effects of PS molecular weight and W_{SM} on dewetting kinetics are explored in detail.

According to the illustration displayed in Figure 1, the initially cast PS/SM films are presumed to possess a highly nonequilibrium morphology wherein copolymer molecules are distributed and self-organized to an unknown extent throughout the PS matrix. Upon annealing, the copolymer molecules self-organize into spherical/cylindrical micelles, channels, or bilayered sheets, depending on blend composition and the ability of the PS molecules to wet the S brush of copolymer aggregate structures. At the copolymer concentrations investigated in this section (W_{SM} up to 0.12), micelles with outlying PS coronas and protected PMMA cores develop. In the PS200/SM blends, the PS molecules are 4× larger than the corresponding block of the copolymer, in which case the coronal brush of the micelles is expected to be dry, i.e., incapable of accommodating PS200 chains within the densely packed S blocks of the copolymer. Annealing the micellar PS200/SM films in the melt provides the micelles, as well as any copolymer molecules remaining dissolved within the PS200 matrix, sufficient thermal energy to migrate[22] to the PS/PMMA interface where the constituent blocks of the copolymer could segregate into their respective phases, reduce the overall free energy of the system, and serve to stabilize the PS200 layer.

The optical images presented in Figure 3 confirm that the initially featureless PS200 layer (Figure 3a) becomes unstable, forming macroscopic holes, upon annealing at 175 °C for ∼24 h (Figure 3b). Further isothermal annealing promotes a systematic increase in hole diameter (D) (Figure 3c−e) until the rims of the holes impinge and ultimately dissociate into discrete droplets (Figure 3f). In our subsequent analysis of dewetting rates (dD/dt) from such images, we only include data from images before rims impinge and hole growth is affected by neighboring holes. Annealing the PS200/PMMA double-layer at higher temperatures (180−190 °C) is found to promote similar dewetting, but at a faster rate. While we have not explored the lower temperature limit at which PS first starts to dewet from PMMA, Costa et al.[13] find that such dewetting occurs at 162 °C. When the SM copolymer is added ($W_{SM} = 0.12$) to the PS200 matrix in the top layer, the film is observed to become stable at 175 °C, exhibiting no evidence of dewetting after being annealed for more than 7 days (Figure 3g). In this case, dewetting only occurs at annealing temperatures above 180 °C (Figures 3h−l), but at a dramatically reduced rate. In Figure 3, hole nucleation sites do not become evident in the PS200/SM layer until the assembly is annealed for ∼47 h. As with the neat PS200 top layer, the dewetting rate of the blended PS200/SM layer increases with increasing temperature (data not shown).

According to the theoretical predictions of Brochard-Wyart et al.,[12] the hole size induced by liquid−liquid dewetting should increase linearly with time when the viscosity (η) of the substrate layer is much higher than that of the top layer so that the bottom layer exhibits solidlike behavior. The PS/PMMA double-layer system investigated in the present work clearly satisfies this prerequisite: η for PMMA281 is estimated[23,24] to be 2.6×10^8 Pa s, whereas η for PS200 is considerably lower[25] 2×10^4 Pa s (by ∼4 orders of magnitude), at 180 °C. While there may be rather large discrepancies in these η values due to the method by which they are estimated, their disparity remains substantial. Figure 4a shows the hole diameter (D) in the neat PS200 layer as a function of annealing time (t) at four different temperatures ranging from 175 to 190 °C, corroborating that linear isothermal hole growth is indeed generally observed in the dewetting of PS on PMMA.[12,26] The constant isothermal dewetting

(22) Schaertl, W.; Tsutsumi, K.; Kimishima, K.; Hashimoto, T. *Macromolecules* **1996**, *29*, 5297.

(23) Wang, C.; Krausch, G.; Geoghegan, M. *Langmuir* **2001**, *17*, 6269.

(24) Fuchs, K.; Friedrich, C.; Weese, J. *Macromolecules* **1996**, *29*, 5893.

(25) Fox, T. G.; Flory, P. J. *J. Am. Chem. Soc.* **1948**, *70*, 2384.

(26) Qu, S.; Clarke, C. J.; Liu, Y.; Rafailovich, M. H.; Sokolov, J.; Phelan, K. C.; Krausch, G. *Macromolecules* **1997**, *30*, 3640.

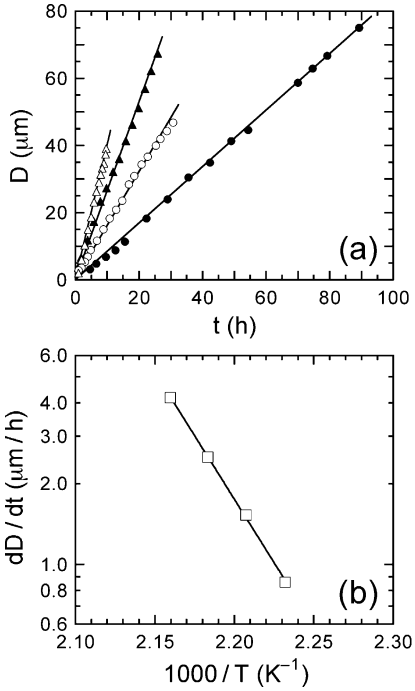

Figure 4. In (a), dependence of dewetted hole size (D) on time (t) for neat PS200 on PMMA281 at four temperatures (in °C): 175 (●), 180 (○), 185 (▲), and 190 (△). The solid lines in (a) denote linear regressions to the data and yield the isothermal dewetting rate constant (dD/dt) at each temperature. In (b), dewetting rate constants as a function of temperature (T) illustrating Arrhenius-type behavior. The solid line in (b) is a fit of eq 4 to the data, which yields an apparent activation energy (E_a) of ∼180 kJ/mol.

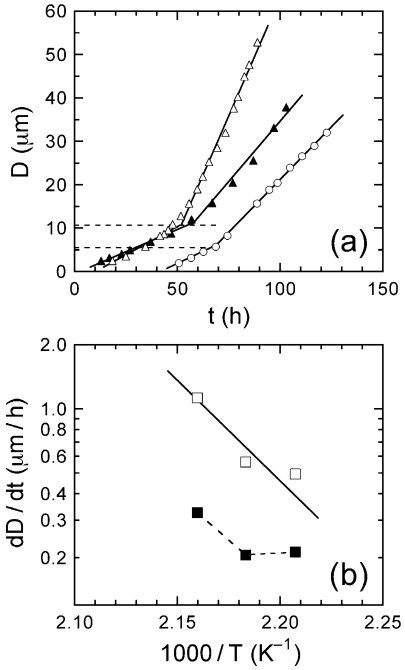

Figure 5. In (a), dewetting kinetics of PS200/SM ($W_{SM} = 0.12$) on PMMA281 at three temperatures (in °C): 180 (○), 185 (▲), and 190 (△). The solid lines in (a) denote linear regressions to the data in early- and late-stage dewetting regimes and yield dD/dt in each regime at each temperature. In (b), the temperature dependence of the early- and late-stage dewetting rate constants (■ and □, respectively). The solid line in (b) corresponds to eq 4 in which E_a is set equal to 180 kJ/mol, whereas the dashed line serves to connect the data.

rates (dD/dt) measured here are further found to increase monotonically with increasing temperature. This dependence can be accurately described by an Arrhenius expression of the form given in eq 4:

$$\mathrm{d}D/\mathrm{d}t = K \exp(-E_a/RT) \qquad (4)$$

where K is a preexponential factor, E_a is the apparent activation energy of homopolymer dewetting, R is the universal gas constant, and T denotes absolute temperature. Regression analysis of the data provided in Figure 4b yields an apparent activation energy of ∼180 kJ/mol. While favorable agreement between the data and eq 4 suggests that PS200 dewetting is a thermally activated process, we recognize that only a very small temperature range has been sampled in this work and that a broader temperature range must be probed to confirm this initial observation.

As illustrated by the images provided in Figure 3, incorporation of the SM block copolymer at a concentration ($W_{SM} = 0.12$) greater than that of the critical micelle concentration (calculated[27] to occur for SM in the PS matrix at $W_{SM} = 0.0097$) into the PS200 layer of the double-layer assembly promotes substantially greater stability relative to the neat PS200 layer due to migration of the copolymer molecules to the PS/PMMA interface and subsequent compatibilization in the melt. Segregation of block copolymer molecules to the PS/PMMA interface can be observed directly by TEM and will be discussed in detail later. A reduction in the interfacial tension between the PS and PMMA layers effectively lowers the driving force for dewetting, in which case it immediately follows that the magnitude of the spreading parameter (S) likewise decreases. While the PS200-rich layer dewets, block copolymer molecules located at the PS/PMMA interface can simultaneously form low-density S brushes capable of interpenetrating with and entangling PS200 chains in the dewetting top layer.[28] It is therefore reasonable to expect that such molecular interpenetration and entanglement significantly increases resistance to dewetting at the PS/PMMA interface. Thus, a combination of decreased driving force for and an increased resistance to dewetting favors greater stability of the PS200/SM layer and consequently lower dewetting rates relative to the neat PS200 layer at temperatures at or above 180 °C.

The time dependence of hole size in PS200/SM layers at three temperatures is plotted in Figure 5a (recall from Figure 3 that the copolymer-modified layer does not dewet at 175 °C). In addition to demonstrating that the added copolymer generally slows hole growth (compare the abscissa ranges in Figures 4a and 5a), these results display a strikingly curious feature: the isothermal dewetting rate exhibits two linear regimes with characteristic constants suggestive of early- and late-stage dewetting processes. Early-stage dewetting is generally slower than that of the accelerated late-stage dewetting, and the crossover from one regime to the other appears to coincide with holes measuring ∼5−10 μm in diameter. Rate constants extracted from the data in Figure 5a are included for comparison in Figure 5b. While the rate constants for both early- and late-stage dewetting are seen to increase with increasing temperature, values of dD/dt determined for late-stage dewetting are far more sensitive to temperature than those corresponding to the early-stage process. While the rate constants measured for late-stage

(27) Hu, W.; Koberstein, J. T.; Lingelser, J. P.; Gallot, Y. *Macromolecules* **1995**, *28*, 5209.

(28) Oslanec, R.; Costa, A. C.; Composto, R. J.; Vlček, P. *Macromolecules* **2000**, *33*, 5505.

dewetting exhibit a modest degree of scatter, the solid line included in Figure 5b (generated from eq 4 with E_a = 180 kJ/mol) represents the data reasonably well and suggests that the activation energy associated with the PS200/SM dewetting process differs little, if at all, from that of neat PS200. This observation further implies that E_a is relatively independent of block copolymer concentration during late-stage dewetting, an unexpected result discussed further later. The physical origin of an apparent crossover from early- to late-stage dewetting in the PS/SM+PMMA double-layer assemblies is not yet known, but may, as considered later, reflect the onset of rims around the dewetted holes or the inability of the high-molecular-weight PS200 molecules to penetrate (wet) the S brush of the copolymer micelles or the copolymer brush that develops at the PS/PMMA interface.

To determine if such crossover is somehow related to homopolymer/copolymer molecular weight disparity, a complementary series of double-layer materials prepared with lower-molecular-weight PS50 and PMMA226 have likewise been investigated. Since η for PMMA226 is reportedly[23−25] much larger than η for PS50, a constant isothermal dewetting rate predicted[12] for dewetting on a solidlike substrate is expected and is indeed observed (cf. Figure 6a) for the neat PS50 layer. Due to the greater mobility of the short PS50 chains relative to that of the long PS200 chains, the dewetting rate is found to be substantially faster, by almost 2 orders of magnitude, for the PS50 layer (114 versus 1.5 μm/h) at 180 °C. Exploratory AFM images acquired from dewetted holes in the PS50 layer after 50 min at 180 °C (data not shown) reveal the persistence of a relatively flat surface, suggesting that the solidlike PMMA substrate undergoes negligible deformation during annealing. Addition of the SM block copolymer to the PS50 layer has a dramatic effect on the dewetting behavior of the layer and appears to be more effective at compatibilizing the PS50/PMMA226, relative to the PS200/PMMA281, interface. At a copolymer concentration of 12 wt % in the PS50 layer, for instance, dewetting does not occur at temperatures as high as 190 °C over a period of 48 h. Recall from Figure 5a that the comparable PS200/SM blend shows evidence of hole formation after ∼50 h at 180 °C.

As alluded to earlier, compatibilization efficacy depends on the relative chain length between the homopolymer molecules and the corresponding blocks of the copolymer.[17] In this blend series, each PS50 molecule is comparable in length to the PS block of the SM copolymer, in which case the homopolymer can penetrate into the copolymer brush and form a wet brush when the copolymer migrates to the PS50/PMMA226 interface. This is not true for the PS200/SM blends, wherein the homopolymer is much longer than the S block of the copolymer. Because of the high entropic penalty required to stretch the blocks in the brush to accommodate the long PS200 chains, a dry brush, which provides less effective compatibilization than a wet one, develops at the PS200/PMMA281 interface. Thus, to probe the dewetting dynamics of PS50/SM layers on PMMA226, we have elected to reduce W_{SM} to 0.03 or less. At these copolymer concentrations, the resultant films dewet over the same temperature range (180−190 °C) encountered in the PS200/SM layers with W_{SM} = 0.12.

Addition of the SM copolymer at the lowest concentration examined here (W_{SM} = 0.01) has a pronounced effect on the dewetting behavior of the PS50 layer, as shown by the dewetting kinetics presented in Figure 6b. These data possess several important characteristics: (i) they all exhibit a single dewetting rate constant under isothermal conditions; (ii) the results obtained at 180 °C indicate that

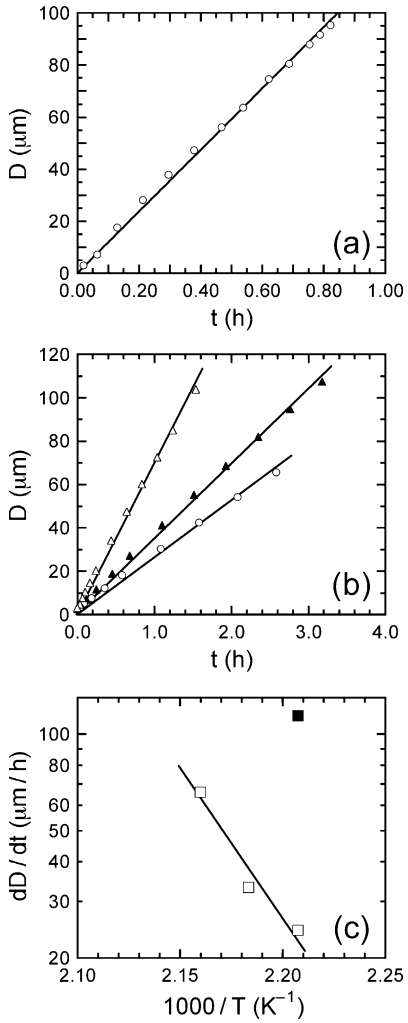

Figure 6. The dewetting kinetics of (a) neat PS50 on PMMA226 at 180 °C and (b) PS50/SM (W_{SM} = 0.01) on PMMA226 at three temperatures (in °C): 180 (○), 185 (▲), and 190 (△). The solid lines in (a) and (b) denote linear regressions to the data and yield dD/dt at each temperature. Values of dD/dt are presented for the neat PS50 (■) and PS50/SM (□) layers as a function of temperature in (c), wherein the solid line corresponds to eq 4 with E_a = 180 kJ/mol.

the PS50/SM layer with 1 wt % copolymer dewets markedly slower (26 versus 114 μm/h) than the neat PS50 layer; and (iii) the dewetting rate increases with increasing temperature. Since all the dewetting kinetics can be assigned a single rate constant, we presume that dewetting occurs by a single process described by the liquid−liquid dewetting model proposed by Brochard-Wyart et al.[12] Isothermal dewetting rate constants extracted from the kinetic data in Figure 6b are displayed as a function of temperature in Figure 6c. As in Figure 5b, a linear regression of eq 4 (with E_a = 180 kJ/mol) to the data in Figure 6c yields unexpectedly favorable agreement and provides additional evidence that the activation energy associated with the (late-stage) dewetting of PS (of at least two different molecular weights) with and without up to ∼12 wt % SM copolymer on PMMA is surprisingly constant. This finding suggests that E_a depends primarily on the chemical constitution, not the molecular weight or (at relatively low W_{SM}) composition, of the two matrix polymers comprising the top layer and substrate and should be relevant to research efforts aimed at designing thin polymer coatings. At higher SM concentrations in the PS50/SM layer (W_{SM} = 0.02 in Figure 7a and W_{SM} = 0.03 in Figure 7b), the dewetting rate not only decreases

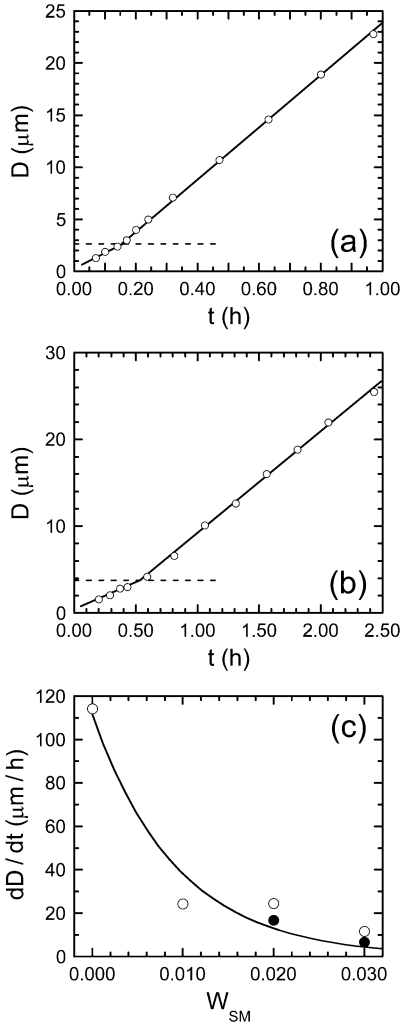

Figure 7. The dewetting kinetics of (a) PS50/SM ($W_{SM} = 0.02$) and (b) PS50/SM ($W_{SM} = 0.03$) on PMMA226 at 180 °C. The solid lines in (a) and (b) denote linear regressions to the data in early- and late-stage dewetting regimes and yield dD/dt in each regime at each temperature. Values of dD/dt for single and late-stage dewetting (○), as well as early-stage dewetting (●), are presented as a function of W_{SM} at 180 °C in (c), wherein the solid line is a fitted exponential function to the data.

but, unlike the PS50/SM blend with only 1 wt % copolymer, also exhibits two different dewetting rate constants similar to the PS200/SM layer ($W_{SM} = 0.12$) in Figure 5a. The crossover from early- to late-stage dewetting, which is more pronounced at 3 wt % SM in Figure 7b, occurs when D is in the vicinity of 3−5 μm (recall that the comparable transition in the PS200/SM double-layer assembly is observed when D lies between about 5 and 10 μm). Isothermal dewetting rate constants ascertained for PS50/SM layers differing in copolymer content from Figures 6b, 7a, and 7b are compared as a function of W_{SM} at 180 °C in Figure 7c and demonstrate that dD/dt decreases nearly exponentially with increasing SM concentration.

Accelerated dewetting of one polymer layer on another has been reported in previous studies. In their investigation of a poly(styrene-*co*-acrylonitrile) (SAN) film dewetting on PS, Segalman et al.[29] have provided results indicating that the dewetting rate increases as holes developed. Pan et al.,[30] likewise observing an increase in the dewetting rate of a polycarbonate (PC) film on a SAN film when the SAN substrate is ultrathin (≤50 nm), propose three possible reasons to explain the incidence of accelerated dewetting: (i) shear-thinning of the top layer, (ii) a change in the dominant energy dissipation mechanism during hole growth, or (iii) a net reduction in the dynamic contact angle. The onset of shear-thinning in the dewetting layer may be responsible for accelerated dewetting in the present work. Recall that two-stage dewetting is only encountered in the PS50/SM and PS200/SM double-layer arrangements and not for either PS50 or PS200. It is reasonable to consider that the shear stress at which neat PS50 or PS200 exhibits shear-thinning (τ^*) might be considerably higher than that induced by dewetting, in which case, shear-induced accelerated dewetting would not be expected to occur in either of the neat PS layers. Addition of the SM copolymer might decrease τ^* sufficiently so that, at some point during annealing, it coincides with the shear stress of dewetting and promotes accelerated dewetting. Moreover, energy dissipation during polymer dewetting is believed[30] to be initially associated with the molten substrate. At later times, however, non-negligible energy dissipation may likewise occur within the hole rim (especially when it becomes high relative to the film thickness).

Another possible explanation for accelerated dewetting is a reduction in indentation depth of the receding rim into the substrate. Several efforts[11,23,29] have established that the top layer indents the substrate under the rim during dewetting. Wang et al.[23] have also shown that the indentation depth decreases when the holes grow to a particular size. It is conceivable that the dewetting rate could change when the indentation depth in the substrate decreases. In our study, however, no evidence of substrate indentation has been observed upon examination of the PS/PMMA interface by AFM (after the top PS or PS/SM layer was selectively removed). In both cases, AFM images confirm the existence of a nearly flat PMMA surface. A pair of representative AFM images illustrating the hole-growth mechanism in a PS50/SM layer ($W_{SM} = 0.03$) annealed at 180 °C for 30 min (near the early- to late-stage crossover in Figure 7a) and quenched to ambient temperature (below the T_gs of PS50 and PMMA226) to freeze-in the dewetted morphology is provided in Figure 8. Numerous holes varying in size are apparent in the layer and reflect different stages of development. At early stages, the layer ruptures to form small holes, the depth of which along the z direction (z is normal to the layer surface) increases with increasing D. As D approaches ∼2 μm, holes with no rims (cf. Figure 8a) reach the high-viscosity PMMA substrate and stop penetrating along z. At later stages of development, rims form around the holes (cf. Figure 8b). These results generally corroborate the two-stage mechanism of hole formation proposed by Green and co-workers.[31,32] In fact, Masson and Green[31] report that the hole size should grow linearly with time (and yield a constant dewetting rate) once the rims are fully developed, which is consistent with the experimental findings reported herein.

Block Copolymer and Dewetting Layer Morphologies. While the primary focus of this work is to establish the effect of SM block copolymer on the dewetting kinetics of PS on a PMMA substrate, we have likewise sought to identify the morphological characteristics of the block copolymer in PS200/SM layers varying in both thickness and W_{SM} and annealed for 7 days at 180 °C under vacuum to achieve near-equilibrium. Following selective staining

(29) Segalman, R. A.; Green, P. F. *Macromolecules* **1999**, *32*, 801.
(30) Pan, Q.; Winey, K. I.; Hu, H. H.; Composto, R. J. *Langmuir* **1997**, *13*, 1758.
(31) Masson, J.-L.; Green, P. F. *Phys. Rev. Lett.* **2002**, *88*, 205504.
(32) Limary, R.; Green, P. F. *Langmuir* **1999**, *15*, 5617.

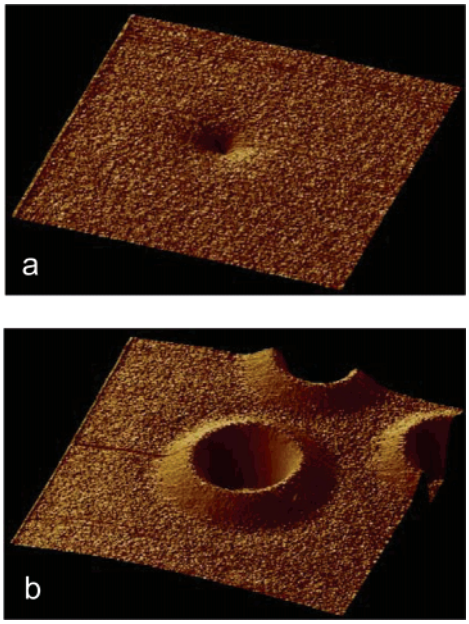

Figure 8. Representative AFM images of holes formed after annealing the PS50/SM layer ($W_{SM} = 0.03$) on PMMA226 for 30 min at 180 °C. The image in (a) displays initial film rupture, whereas the one in (b) reveals fully formed rims around the holes. The image sizes are 20 and 50 μm in (a) and (b), respectively.

of the styrenic moieties (to enhance their electron contrast), these thin PS200/SM+PMMA double-layer assemblies are suitable for direct examination by TEM. Figure 9 shows several representative images of the macroscopic and microscopic morphologies observed in these assemblies. The macroscopic morphology of the top PS200/SM layer ranges from nondewetted to the formation of discrete PS200-rich islands and filaments, depending on both copolymer concentration and layer thickness. Figure 10 summarizes the dependence of these morphologies on copolymer concentration and film thickness, and confirms that thick films possessing a high SM concentration tend to be more stable. In addition to the macroscopic morphology of these systems, close examination of images such as the one presented in Figure 9a reveals the existence of SM micelles. Micelles with a stained S corona and an unstained M core measuring 40 ± 4 nm in diameter form in relatively thick PS 200 films that do not show signs of dewetting. A reduction in layer thickness to below a critical value (~50 nm) precludes micelle formation due to the high entropy penalty arising from geometric confinement.[18]

Dewetting of the PS200/SM layer and the subsequent formation of islands (Figure 9b) on the PMMA substrate favor formation of SM micelles due to a local increase in layer thickness and correspondingly reduced confinement. During the dewetting process, it is reasonable to expect that some of the SM molecules and possibly entangled PS200 molecules will be deposited on the PMMA surface behind the receding contact line. In numerous instances, noncontinuous, S-containing filaments (represented by Figure 9c) that appear to be molecularly thin reside between dewetted islands, whereas nanoscale droplets similar to those reported by Green and Ganesan[33] for PS on an inorganic substrate are observed in others (cf. Figure 9d and e). One possible explanation for the nanoscale droplets in the present study is that copolymer molecules residing in micelles within the PS200/SM layer may either retain their organization as surface (hemispherical) micelles or disorganize to form brushes upon exposure to the PMMA281 surface. In Figure 9d and e, the discrete nanoscale dispersions measure 51 ± 11 nm in diameter on the unstained PMMA. If some of these features correspond to corona-stained SM micelles that have not undergone severe deformation at the PS/PMMA interface, then the core diameter and corona thickness can be determined by comparing the sizes of the micelles in the PS200/SM layer and those residing on the PMMA281 surface. These dimensions discerned from images such as those displayed in Figure 9 are ~40 nm (M core diameter) and ~11 nm (S coronal thickness). Corresponding gyration diameters estimated for M and S Gaussian coils of comparable molecular weight (as the blocks in the copolymer) are 14.4 and 12.5 nm, respectively, indicating that the M blocks are slightly stretched, while the S blocks are collapsed.

The surface features visible in Figure 9d and e provide evidence to suggest that block copolymer molecules individually and as ensembles migrate through the PS200/SM layer to the PS200/PMMA281 interface. Once there, the blocks of dissolved molecules can segregate into their compatible phase, whereas micelles would first have to adsorb and open to some extent to form a surface micelle. Complete dissolution of an adsorbed SM micelle would result in the formation of a copolymer brush, which would interpenetrate (albeit very little due to the homopolymer/copolymer molecular weight disparity previously discussed) the adjacent homopolymer matrices, reduce interfacial tension, and promote greater stability of the PS200/SM layer relative to the neat PS200 layer. Another factor that must be considered in light of the evidence provided in Figure 9 is interfacial roughness. If SM micelles migrate to the interface and remain intact or merge to form a continuous morphology such as a microemulsion[18] (Figure 9f), they will undoubtedly affect interfacial roughness, which, as reported elsewhere,[1] would further slow the rate of dewetting. Thus, addition of a block copolymer to a dewetting homopolymer layer in a double-layer arrangement may alter (i) the system thermodynamics by effectively reducing the interfacial tension (i.e., the driving force for dewetting) as copolymer molecules locate at the polymer/polymer interface and (ii) the system dynamics by altering interfacial roughness due to micelle adsorption or a subsequent morphological transformation.

Conclusions

While most experimental studies of polymer dewetting have focused on homopolymer or block copolymer films deposited on a solid (impenetrable) surface such as silicon, we have examined the kinetics of PS/PMMA dewetting when the top PS layer is modified by the addition of an SM diblock copolymer. Neat PS is shown to dewet from PMMA by nucleation and growth when the double-layer assemblies are annealed in the melt at temperatures well above the T_gs of PS and PMMA. The isothermal dewetting rate in this case is found to be constant, in agreement with theoretical predictions,[12] and increases with increasing temperature. The dewetting rate is also sensitive to PS molecular weight, increasing markedly with decreasing molecular weight. Addition of the SM copolymer to the PS layer greatly increases the stability of the film by either slowing the rate of dewetting or, at sufficiently high concentrations, altogether preventing dewetting at a given temperature. In the latter case, the onset temperature of dewetting can be controllably adjusted via judicious choice of copolymer content. Such stabilization is attributed to

(33) Green, P. F.; Ganesan, V. *Euro. Polym. J.*, in press.

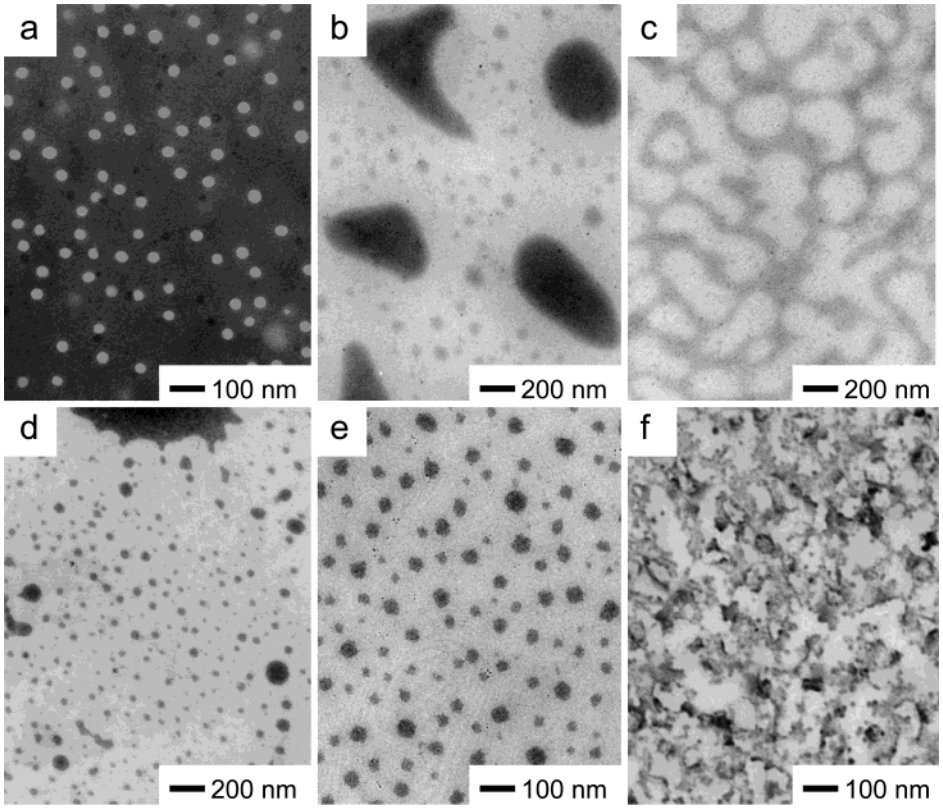

Figure 9. TEM images of some of the morphologies observed in PS200/SM+PMMA281 double-layer assemblies varying in W_{SM} and film thickness (L, in nm) after annealing at ~180 °C for 7 days (expressed in terms of W_{SM}, L): (a) 0.24, 88; (b) 0.48, 10; (c) 0.12, 74; (d) 0.04, 13; (e) 0.04, 37; and (f) 0.12, 57. Bulk micelles in the PS200 layer appear as bright features due to the unstained PMMA core, whereas dewetted islands and surface micelles/brushes residing at the dry PMMA281 surface appear as dark features due to the RuO_4-stained PS corona.

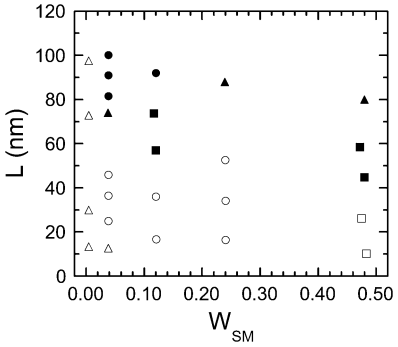

Figure 10. Experimental morphology diagram (expressed in terms of L and W_{SM}) of the PS200/SM layer on the PMMA281 substrate after annealing at ~180 °C for 7 days: nondewetted PS200/SM layer with bulk SM micelles (●), weakly dewetted PS200/SM layer with bulk SM micelles (▲), finely connected PS200/SM filaments (■), connected PS200/SM islands with surface SM micelles (○), isolated PS200/SM islands with surface SM micelles (△), and discrete PS200/SM islands with bulk and surface SM micelles (□).

interfacial compatibilization, which becomes increasingly more effective as the molecular weights of the homopolymers and corresponding blocks of the copolymer converge and the densely packed blocks of the copolymer molecules can be penetrated to form wet brushes.

An interesting feature observed here is that, again at sufficiently high copolymer concentrations, the isothermal dewetting rates are not constant, thereby providing evidence of early- (slow) and late-stage (accelerated) dewetting regimes. The onset of accelerated dewetting coincides with holes of a particular size and may be related to rim development. Isothermal dewetting rate constants measured from the late-stage regime are more sensitive to temperature variation than those discerned from the early-stage. The morphological characteristics of annealed double-layer assemblies have been investigated by TEM and reveal that the macroscopic and microscopic details depend on both copolymer concentration and film thickness. Relatively thick PS/SM films possessing a high block copolymer concentration exhibit very little, if any, dewetting but form SM micelles within the PS layer. The micelles also reside in dewetted PS regions at reduced copolymer concentrations and film thicknesses. In these cases, discrete dispersions residing on the dry PMMA surface are attributed to surface-adsorbed micelles or unraveled SM brushes. One final observation of this study that warrants mention is that prolonged exposure of these PS/SM+PMMA double-layer assemblies to visible light or UV radiation can systematically affect not only the dewetting rate but also the resultant morphology of the PS/SM layer at elevated temperatures (see the Appendix). The precise reason for this phenomenon is not yet clear, but research efforts devoted to elucidating polymer dewetting mechanisms should be aware of this possible source of concern.

Appendix

An unexpected outcome of the present study is the observation that the final dewetted layer morphology is significantly affected by prolonged exposure to light. A series of PS200/SM films ($W_{SM} = 0.12$) has been annealed on PMMA281 at 180 °C and monitored continuously by optical microscopy in reflection mode. As illustrated in Figure 2, the light of the microscope incessantly shines on the same specimen area. Over the course of 4 days, the dewetting process is observed to remain unaffected, with

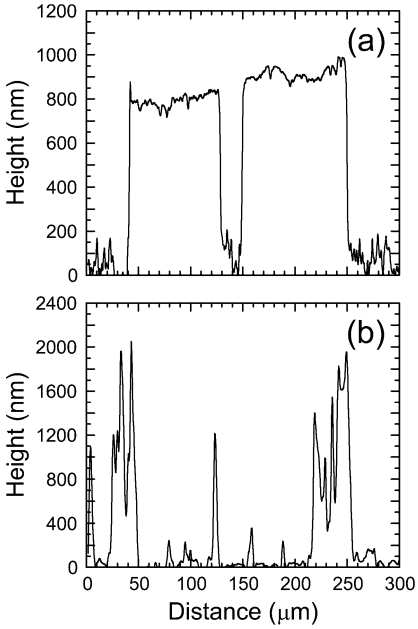

Figure 11. Profilometry of dewetted PS200/SM islands on PMMA281 (a) with and (b) without exposure to visible light during annealing for 6 days at 180 °C.

illuminated and nonilluminated regions of the layer appearing to be virtually identical. However, at longer times (after 5 or 6 days), microscopic features, such as holes, rims, and islands, in the illuminated area become irresolvable, in marked contrast to comparable features that remain clearly visible in surrounding nonilluminated areas. Upon removal of the assembly from the hot-stage, a circular dark area is visually discernible by the unaided eye. To ensure that this observation does not arise due to a difference in experimental conditions, all tests have been reproduced with continuous light of constant intensity. Surface features of illuminated and nonilluminated specimen areas discerned by profilometry are depicted in parts a and b of Figure 11, respectively. Dewetted islands inside the illuminated area are generally large and measure ~80 nm high, whereas those outside the exposed area tend to be smaller and as high as ~200 nm. Hole rims observed in complementary AFM images of nonilluminated specimens measure up to 400 nm in height. Thus, prolonged light exposure appears to influence the morphology of the dewetted PS200/SM layer. This curious phenomenon is not observed at annealing temperatures of 185 °C and above because of accelerated dewetting. To corroborate the effect of light on dewetting behavior, a UV source (wavelength = 365 nm) has been employed as a substitute for visible light. The results from this UV test are strikingly similar to those observed using white light with a noticeable exception: the area subjected to UV radiation appears irresolvable after a substantially shorter exposure time (only 2 days).

Careful observation of images collected from double-layer assemblies affected by light reveals that the wetted PS200/SM layer areas, not the dry patches in dewetted holes, become obscured at late annealing times (day 5 or 6 for visible light and day 2 for UV radiation). Further annealing significantly decreases the contrast between the holes/rims and the background, thereby resulting in reduced feature delineation. The reason for this light-induced effect remains an open question, but it should be considered further since it profoundly impacts accurate assessment of dewetting kinetics. We suggest that light exposure might trigger a dewetting mechanism other than the nucleation-and-hole mode in specimen areas that are subject to further dewetting. This mechanism may be related to a spinodal-like dewetting process, wherein features form at length scales below the resolution limit of the optical microscope. Moreover, it may be triggered only after a sufficiently high light dosage is achieved for a particular temperature. Segalman et al.[29] have reported the occurrence of spinodal dewetting in a SAN layer measuring 100 nm thick on a PS substrate. In their study, they find evidence of an interconnected intermediate morphology with a characteristic length scale of ~10 μm. Spinodal-like dewetting of SAN on a hard (silicon) substrate has likewise been documented.[34] Another possibility to be considered is that extended light exposure might adversely affect the PMMA layer that becomes increasingly exposed as the top PS200/SM layer dewets. It is well-established, for instance, that long-wavelength (~350 nm) UV radiation can not only degrade PMMA[35] but also induce cross-linking and chain scission in PS.[36] While we have listed some possible explanations that might help to elucidate the origin of the anomalous effects described above, a detailed analysis of this phenomenon is beyond the scope of the present work, but certainly warrants future investigation.

Acknowledgment. This work was supported by the Kenan Institute for Engineering, Technology, and Science at North Carolina State University. We thank Dr. J. J. Semler for technical assistance and advice.

LA049562C

(34) Masson, J.-L.; Green, P. F. *J. Chem. Phys.* **2000**, *112*, 349.
(35) Reiser, A. *Photoreactive Polymers, the Science and Technology of Resists*; John Wiley & Sons: New York, 1989.
(36) Thurn-Albrecht, T.; Schotter, J.; Kästle, G. A.; Emley, N.; Shibauchi, T.; Krusin-Elbaum, L.; Guarini, K.; Black, C. T.; Tuominen, M. T.; Russell, T. P. *Science* **2000**, *290*, 2126.